1 **SUPPLEMENTARY FIGURES**

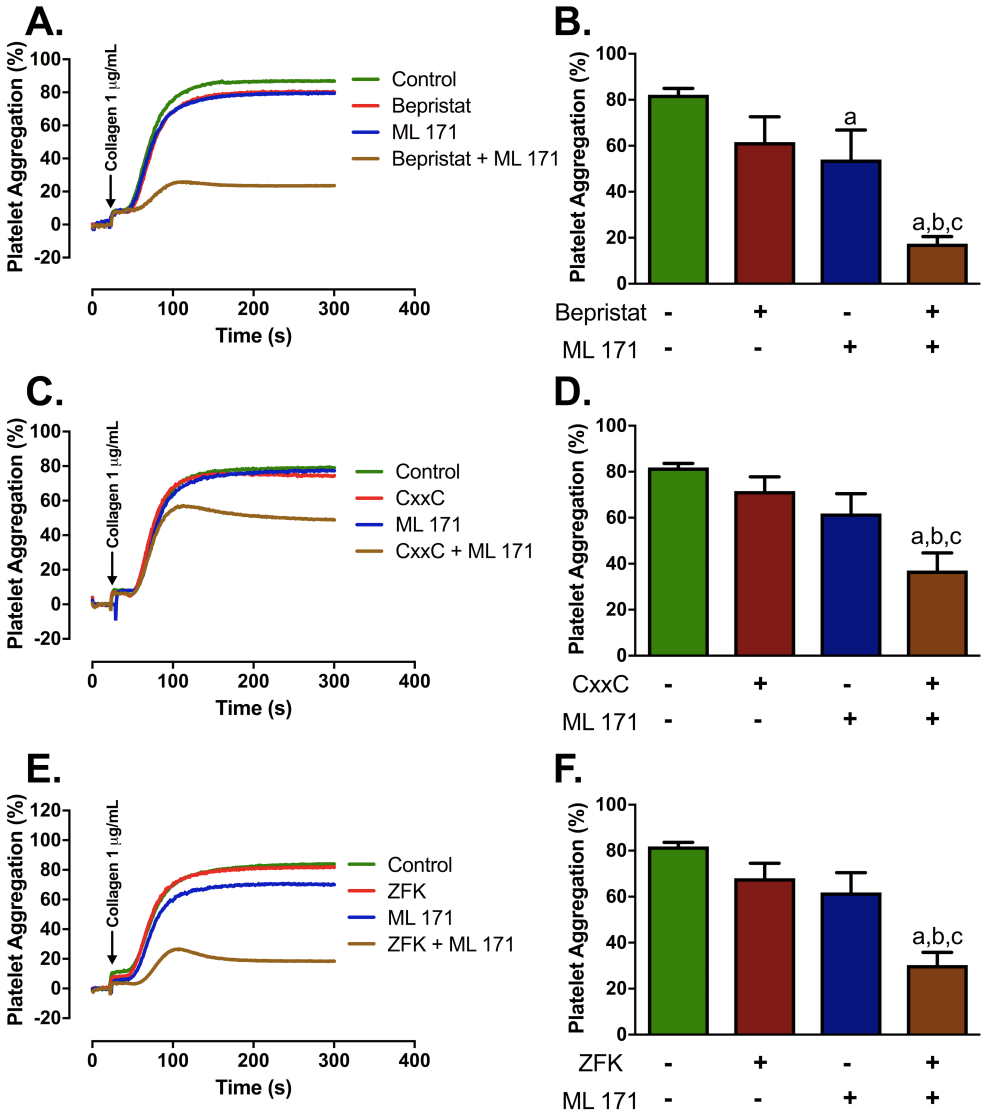

2

3 **Supplementary Figure 1. Different PDI inhibitors exert similar additive**
4 **inhibitory effect to ML171 in turbidimetry platelet aggregation induced by**
5 **Collagen.** Human WP at 4 x 10^8 platelets/mL were incubated with 0.75 µM ML171
6 and/or: 15 µM Bepristat (A) and (B), 50 µM CxxC peptide (C) and (D) or 1.25 µM
7 Zafirlukast for 10 minutes, then stimulated with 1µg/mL Collagen. Aggregation traces
8 were recorded for up to 5 minutes. Representative aggregation curves are provided in
9 (A), (C) and (E) with corresponding summary statistics in (B), (D) and (F). n=3-5
10 different donors. Data on graphs show mean ± SEM. Data analysed by paired one-
11 way ANOVA with Tukey's post-test. a $p<0.05$ *vs* first column; b $p<0.05$ *vs* second
12 column and c $p<0.05$ *vs* third column of corresponding graph.

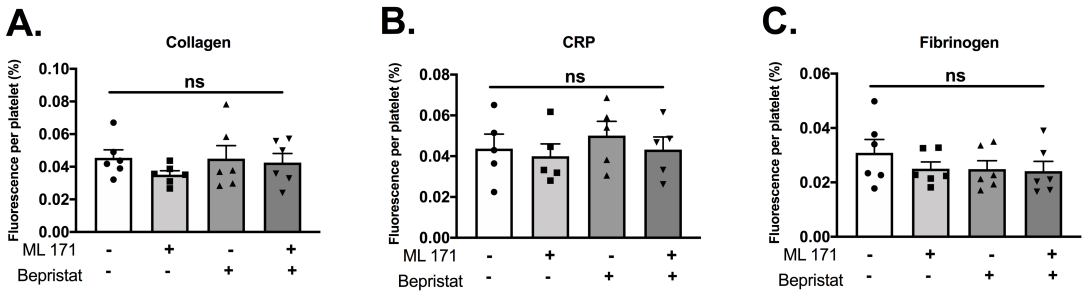

Supplementary Figure 2. No additive inhibitory effect of bepristat and ML171 on human platelet spreading. Human WP at 2 x 10^7 platelets/mL were incubated with ML171 (3 μM) and/or bepristat (15 μM) for 10 minutes and left to adhere and spread on Collagen- (A), CRP- (B) or Fibrinogen-coated (C) surfaces for 45 minutes. Platelets were labeled with fluorescently tagged phalloidin and visualized in a Nikon A1-R confocal microscope. Number of adhered platelets was divided by total fluorescence of field to obtain fluorescence per platelet as a surrogate for platelet spreading. Data on graphs show mean ± SEM. Data analysed by paired one-way ANOVA with Tukey's post-test. ns: $p>0.05$.

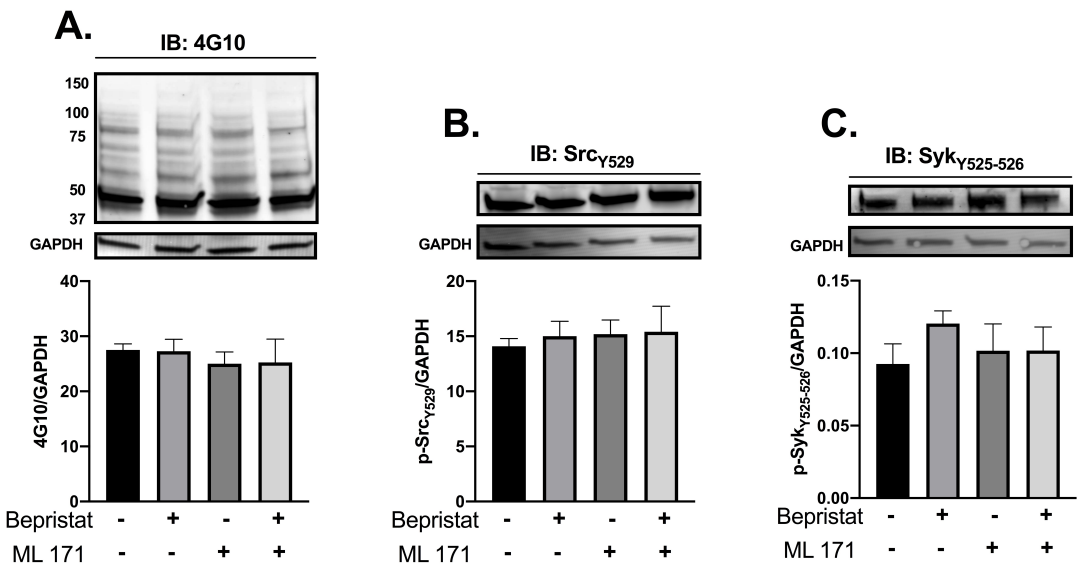

Supplementary Figure 3. PDI and Nox-1 co-inhibition did not affect tyrosine phosphorylation or phosphorylation of upstream GPVI proteins. WP at 4 x 10^8 platelets/mL were incubated with 3 μM ML171 and/or 15 μM bepristat for 10 minutes prior to the addition of 3 μg/mL Collagen. Platelets were lysed after 90 seconds and immunoblots performed. Samples were tested for: 4G10 total Tyr phosphorylation (A), Src Y529 (B) and Syk Y525-526 (C). Representative blot is presented on top of bar graphs with summary statistics. Each lane represents the condition in graph below. n=3-4 donors. Data on graphs show mean ± SEM and analysed by paired one-way ANOVA and Tukey's post-test.

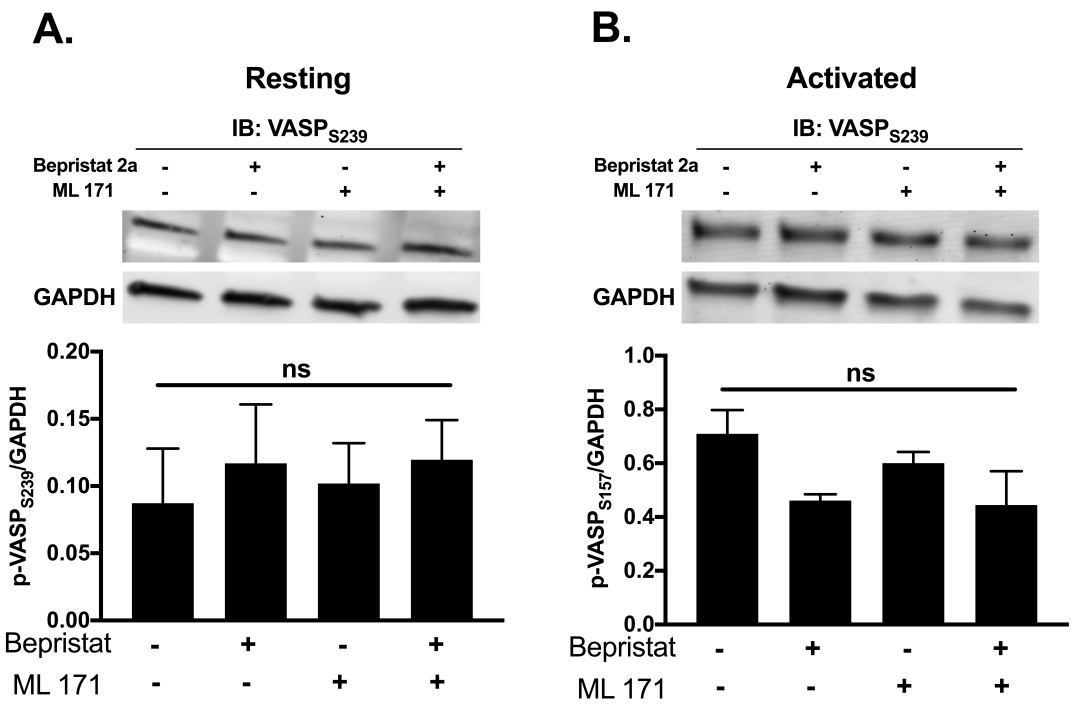

Supplementary Figure 4. VASP phosphorylation in resting and activated platelets was not affected by PDI and Nox-1 inhibition. WP at 4 x 10^8 platelets/mL were incubated with 3 μM ML171 and/or 15 μM bepristat for 10 minutes prior to the addition of 3 μg/mL collagen. Some collagen-stimulated samples were treated with vehicle alone. Platelets were lysed after 90 seconds and immunoblots performed. Samples were tested for VASP S239 phosphorylation. Representative blot is presented on top of bar graphs with summary statistics. Each lane represents the condition in graph below. n=3-4 donors. Data on graphs show mean ± SEM and analysed by paired one-way ANOVA and Tukey's post-test.

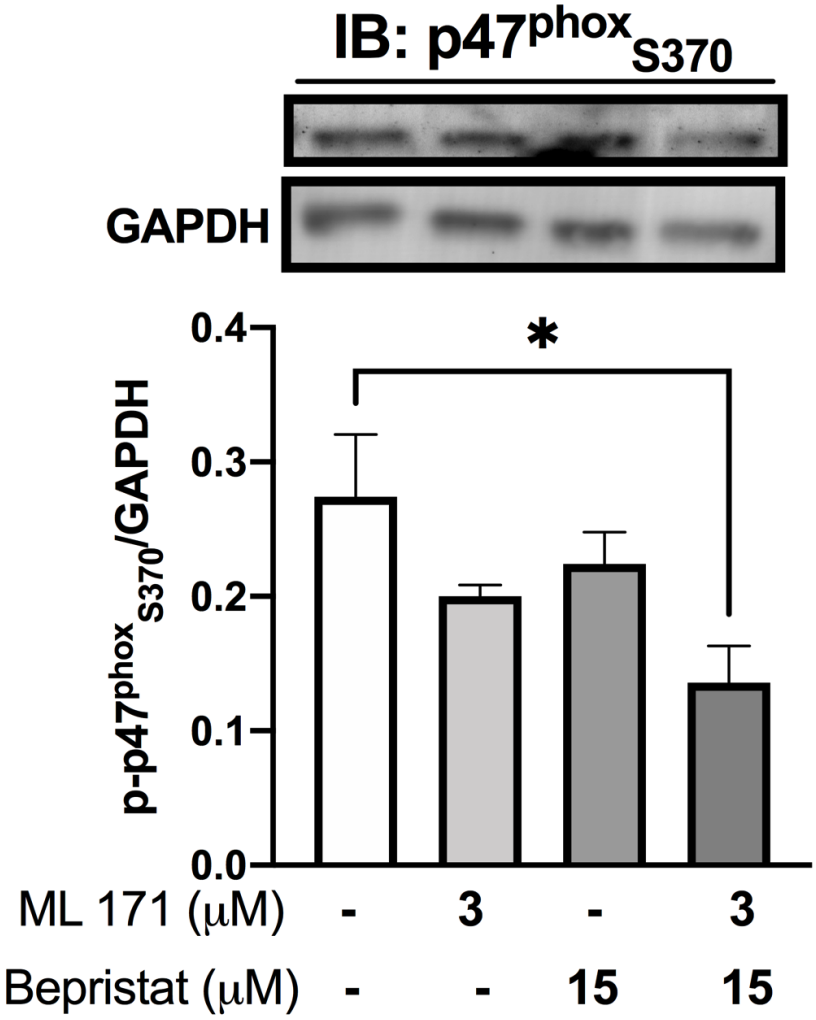

Supplementary Figure 5. PDI and Nox-1 co-inhibition decreases phosphorylation of p47phox. WP at 4 x 10^8 platelets/mL were incubated with 3 μM ML171 and/or 15 μM bepristat for 10 minutes prior to adding 3 μg/mL Collagen. Platelets were lysed after 90 seconds and immunoblots performed. Samples were tested for phosphorylation of p47phoxS370. GAPDH was used as a control for equal loading. Representative blot is presented above of bar graph with summary statistics, following normalisation for protein loading. Each lane represents the condition in graph below. Data are representative of 3-4 independent experiments. Bar graph shows mean ± SEM and was analysed by paired one-way ANOVA and Tukey's post-test. * $p<0.05$.

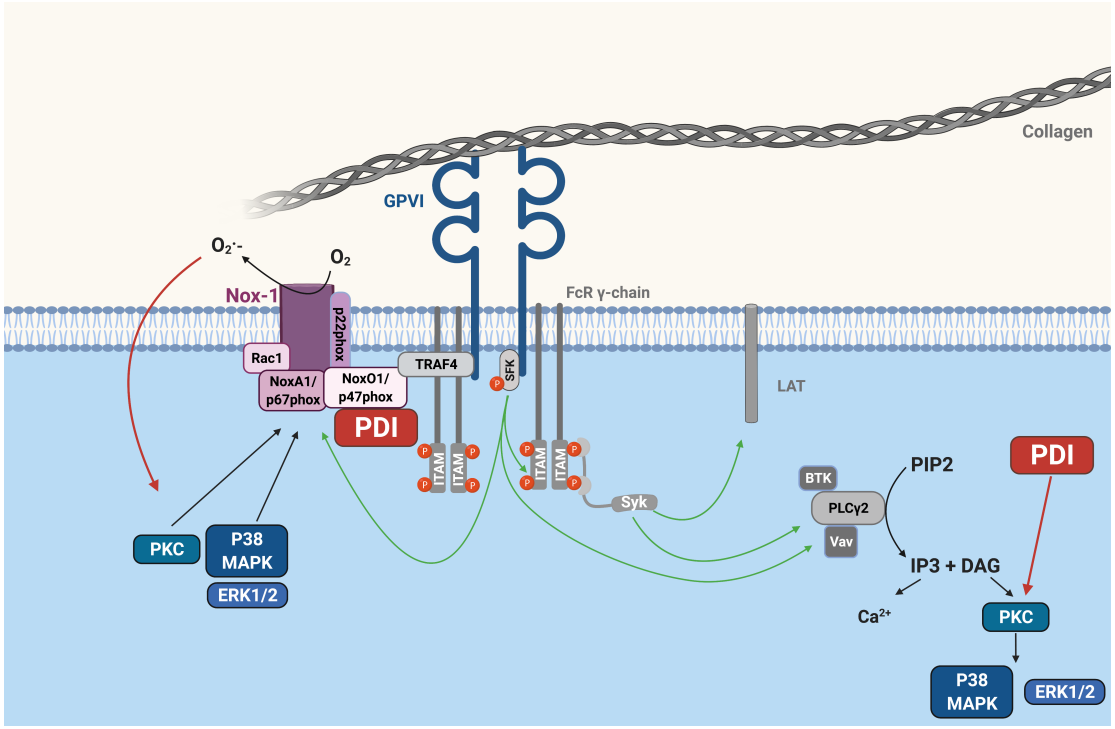

Supplementary Figure 6. Summary of molecular processes regulated by PDI and Nox-1 in collagen-mediated signal. Upon collagen binding to clustered or dimeric glycoprotein VI (GPVI), the cytosolic tail of GPVI activates Src family kinases (SFK) which phosphorylate the immunoreceptor tyrosine-based activation motif (ITAM) part of the Fc receptor γ-chain, Bruton's tyrosine kinase (BTK), and lead to activation of the Nox-1 complex that is attached to GPVI through TNF receptor-associated factor 4 (TRAF4). PDI localizes with p47phox upon activation with CRP. BTK will phosphorylate phospholipase C (PLCγ2). ITAM phosphorylation results in activation of Syk, which will phosphorylate linker for activation of T cells (LAT) protein, as well as PLCγ2, Vav and BTK. PLCγ2 will catalyse the formation of trisphosphate inositol (IP3) and diacylglycerol (DAG) from phosphatidylinositol 4,5-bisphosphate (PIP2). PIP2 may be converted to phosphatidylinositol-3,4,5-trisphosphate (PIP3) by phosphoinositide 3-kinase (PI3K). IP3 and DAG will increase intracellular Ca2+ and induce protein kinase C (PKC) activation, which will phosphorylate mitogen-activated protein kinases (MAPK). PDI regulates the activation of PKC and MAPKs, which interact with p47phox to assemble the Nox-1 complex that is responsible for superoxide generation. Superoxide may then activate PKC and MAPKs in a positive feedback loop. Green lines indicate early GPVI signalling.

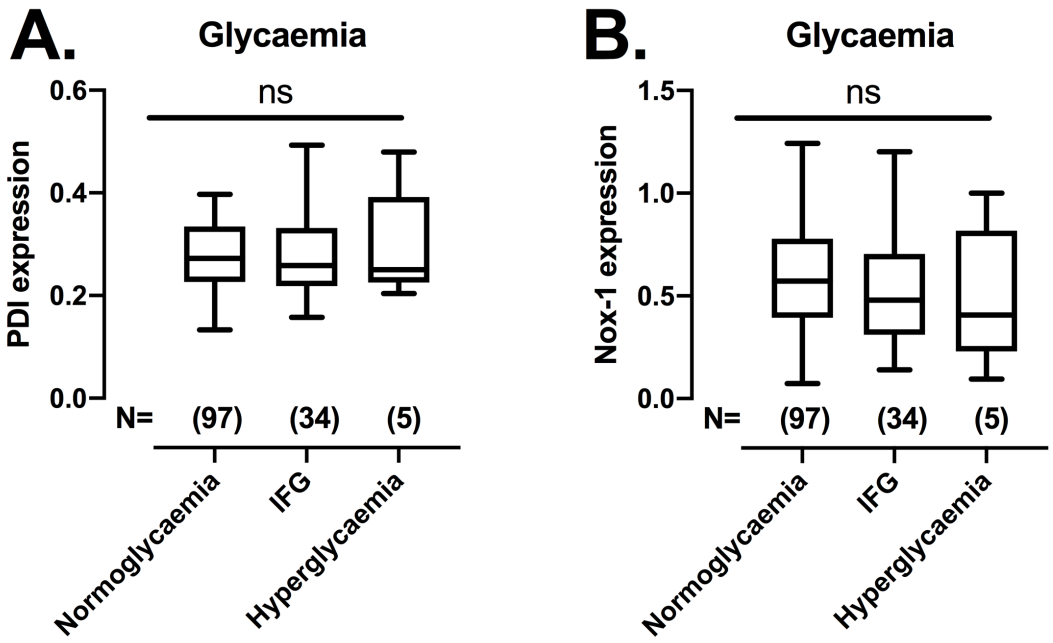

Supplementary Figure 7. Platelet PDI and Nox-1 are not increased in hyperglycaemia. Washed platelets (WP) from 136 volunteers were lysed and immunoblots performed for PDI, Nox-1 and loading control GAPDH. Anthropometric and metabolic characteristics were also collected. Value cut-offs of stratifications can be found on Supplementary Methods and were all performed according to international guidelines. PDI and Nox-1 expression were stratified by: (A and B) glycaemia in normoglycaemia (<5.6 mmol/L), impaired fasting glycaemia (IFG) (5.6 – 6.9 mmol/L) and hyperglycaemia (>6.9 mmol/L). Data in graph show box and whiskers depicting median, range and 25th and 75th percentiles analysed by one-way ANOVA and Tukey's post-test. ns: $p>0.05$.

91 **SUPPLEMENTARY TABLES**

92 **Supplementary Table 1. Full blood count of WT and Nox-1$^{-/-}$ mice**

	WT	Nox-1$^{-/-}$
Red Blood Cells		
Hematocrit (%)	36.67±1.368	36.00±0.806
RBC (x10^3/µL)	7.76±0.278	7.67±0.192
Haemoglobin (g/dL)	12.42±0.504	12.30±0.158
MCV (fL)	47.37±0.214	47.50±0.65
MCH (pg)	15.89±0.155	16.04±0.287
MCHC (g/dL)	33.54±0.336	34.20±0.626
RDW (%)	14.64±0.148	**15.64±0.256***
White Blood Cells		
Leukocytes (x10^3 cells/µL)	6.75±0.247	**8.22±0.407***
Lymphocytes (x10^3 cells/µL)	5.47±0.337	**6.82±0.296***
Lymphocytes (%)	82.92±1.216	82.94±0.618
Monocytes (x10^3 cells/µL)	0.76±0.072	0.82±0.066
Monocytes (%)	9.52±0.571	9.98±0.392
Granulocytes (x10^3 cells/µL)	0.60±0.072	0.60±0.071
Granulocytes (%)	8.50±1.136	7.08±0.41
Platelets		
Platelet count (x10^3 cells/µL)	507.9±22.78	468.8±20.49
MPV (fL)	4.95±0.043	4.98±0.111

93 Data presented as mean ± SEM. N= 7 mice for WT and N=5 for Nox-1$^{-/-}$. Groups were compared by
94 unpaired Student t-test. * $p<0.05$.

95

96

97 **Supplementary Table 2. Summary statistics of study population (n=137)**

Parameter	
Age (years)	48.08 ± 11.46
BMI (kg/m^2)	25.09 ± 4.15
Gender (M%/F%)	(32%/68%)
Glycaemia (mmol/L)	5.36 ± 0.70
Systolic BP (mmHg)	128.3 ± 15.15
Waist (cm)	88.18 ± 11.13
PDI expression	0.27 ± 0.07
Nox-1 expression	0.57 ± 0.27

98 Data presented as mean ± SD or % for gender. BMI: body mass index. BP: blood pressure. PDI:
99 protein disulphide isomerase. Nox-1: NADPH oxidase-1.
100

101 **SUPPLEMENTARY METHODS**

102 **1. Reagents**

103 Prostacyclin (PGI_2), Bepristat 2a, Zafirlukast, Phorbol-12-myristate-13-acetate
104 (PMA), Thrombin Receptor Activator Peptide 6 (TRAP-6), human fibrinogen and
105 3,3′-Dihexyloxacarbocyanine iodide ($DIOC_6$) were purchased from Sigma-Aldrich
106 (Dorset, UK). PAPA-NONOate and ML171 (also known as 2-acetylphenothiazine or
107 2APT) was purchased from Tocris (Abingdon, UK). PE/Cy5 anti human CD62P
108 antibody was purchased from BD Biosciences (Wokingham, UK). FITC-conjugated
109 fibrinogen was purchased from Agilent (Stockport, UK). PDI inhibitor CxxC peptide
110 [1] was purchased from EZBiolab (Parsippany, USA). GFOGER was purchased from
111 CambCol (Cambridge, UK). Collagen was purchased from Nycomed (Munich,
112 Germany) whereas Collagen-Related Peptide (CRP) was obtained from Prof Richard
113 Farndale (University of Cambridge, Cambridge, UK). Anti-PDI (NB600-1164, clone
114 RL77), Anti-Nox-1 (NBP1-31546) were from Novus Biologicals (Bio-techne R&D
115 Systems Europe Ltd, Abingdon, UK). Anti-p47phox, anti-phospho p47phox Ser370,
116 4G10 total phospho Tyr, Fura-2 AM calcium dye, Alexa-488, Alexa-568 and Alexa-
117 647-conjugated secondary antibodies were bought from ThermoFisher (Paisley, UK).
118 Anti-ERK1/2 and anti-p38 antibodies were purchased from Santacruz Biotechnology
119 (Heidelberg, Germany). Anti-Akt, anti-phospho Src Tyr529, anti-phospho Syk
120 Tyr525/526, anti-phospho vasodilator-stimulated phospho-protein (VASP) (Ser239),
121 PKC substrate, anti-phospho-Akt Ser473, anti-phospho p38 Thr180/Tyr182, anti-
122 phospho ERK Thr202/Tyr204 were purchased from Cell Signalling (Hitchin, UK).
123 Anti-glyceraldehyde 3-phosphate dehydrogenase (GAPDH) was purchased from
124 Proteintech (Manchester, UK).

125

126 **2. Washed platelets preparation**

127 Blood was collected from healthy adult volunteers who were not using
128 antiplatelet medication and had previously provided informed consent. Platelet-rich
129 plasma (PRP) was obtained after centrifuging whole blood at 100 x *g*, 20 minutes,
130 22°C. To obtain washed platelets (WP), PRP was centrifuged twice at 1000 x *g*, 10
131 min, 22°C in the presence of 1.25 µg/mL prostacyclin and 1:5 v/v acid citrate
132 dextrose (ACD: 5% sodium citrate, 2% D-glucose and 1.5% citric acid). The final
133 platelet pellet was resuspended in modified Tyrode's-HEPES buffer, (134 mM NaCl,
134 20 mM N-2-hydroxyethylpiperazine-N′-2-ethanesulfonic acid, 12 mM $NaHCO_3$ 5

135 mM glucose, 0.34 mM Na_2HPO_4, 9 mM KCl and 1 mM $MgCl_2$, pH 7.3) and rested
136 for 30 minutes at 30 °C before experiments. The Research Ethics Committee from the
137 University of Reading approved all protocols to obtain and use human blood samples.
138
139 **3. Collection of mouse blood and platelet preparation**
140 Colonies of Nox-1$^{-/-}$ mice were purchased from Jackson Laboratory
141 (Sacramento, CA, USA) and C57BL/6 were used as controls, as recommended by the
142 animal provider. Animals were kept under a 12 h light cycle, controlled temperature
143 (22-24°C) and food and water *ad libitum*. The University of Reading Local Ethics
144 Review Panel approved all protocols within a license from the British Home Office.
145 Mice (11 – 14 weeks, females) were culled in a CO_2–filled chamber and blood
146 collected through cardiac puncture in a syringe containing 3.2% sodium citrate at a
147 1:9 v/v citrate-blood ratio. Whole blood was centrifuged at 203 x *g* for 8 minutes and
148 PRP collected. 1.25 µg/mL PGI_2 was added and PRP centrifuged at 1,028 x *g* for 5
149 min and pellet resuspended in modified Tyrode's-HEPES buffer to obtain WP.
150
151
152 **4. Immunofluorescence microscopy**
153 Human PRP were activated with 1 µg/mL CRP for 3 minutes in the presence
154 of integrillin at 4 µg/mL. PRP was fixed immediately using 5% paraformaldehyde and
155 centrifuged at 1000 x *g* for 10 minutes. The pellet was resuspended in 1:9 v/v ACD-
156 phosphate buffer solution (PBS) and submitted to another centrifugation under the
157 same conditions. The final pellet was resuspended in PBS containing 1% w/v BSA
158 and left to adhere onto poly-L-lysine coverslips for 90 minutes at 37 °C. Coverslips
159 were washed three times with PBS and blocked again in PBS containing 1% w/v BSA
160 for 1 hour. Blocking buffer was washed away with PBS and primary or IgG control
161 antibodies added at 1:250 v/v dilution in PBS containing 0.2% v/v Triton-X-100 and
162 2% v/v donkey serum and incubated at 4 °C overnight. Antibodies were washed away
163 three times with PBS and appropriate secondary antibodies tagged with different
164 fluorophores added for 1 hour at room temperature. Finally, coverslips were mounted
165 in gold anti-fade onto a coverslips and analysed with a 100 x magnification oil-
166 immersion lens on a Nikon A1-R confocal microscope (Nikon Instruments Europe
167 BV, Amsterdam, Netherlands).
168

169 **5. Turbidimetry and plate-based platelet aggregation**

170 Platelet aggregometry was performed by turbidimetry in a four-channel
171 AggRam aggregometer (Helena Biosciences, Gateshead, UK), as described
172 previously [2]. Briefly, human (4 x 10^8 platelets/mL) or mouse (2 x 10^8 platelets/mL)
173 WP were pre-incubated with inhibitors for 10 minutes before stimulation with
174 collagen and curves recorded for up to 300 seconds. For mouse experiments, WP
175 were pre-incubated with inhibitors for 10 minutes and stimulation obtained with 5
176 μg/mL collagen. The concentrations of inhibitors used are described in appropriate
177 figure legend. To reconstruct the curves, 0% was set when t = 10 seconds and 100%
178 set as blank (distilled water) placed at the end of the run in each channel for at least
179 15 seconds.

180 Platelet aggregation was also assessed through an end-point, plate-based
181 method, as described previously [3]. Briefly, human WP (4 x 10^8 platelets/mL) were
182 added to a 96-wells half-area plate (Greiner) containing varying concentrations of PDI
183 inhibitor Bepristat or Nox-1 inhibitor ML171 and incubated for 10 minutes. Then,
184 agonists collagen (2 μg/mL), CRP (1 μg/mL), TRAP-6 (10 μM) or PMA (500 nM)
185 were added and plate shaken at 1200 rpm for 5 minutes at 37°C using a plate shaker
186 (Quantifoil Instruments). Absorbance was measured at 450 nm using a Flexstation 3
187 plate reader.

188

189 **6. Fibrinogen binding and P-selectin exposure**

190 Human WP (4 x 10^8 platelets/mL) were incubated with 7.5 μM Bepristat
191 and/or 0.75 μM ML171 for 10 minutes. Platelets were activated with 1 μg/mL CRP
192 for 10 minutes and incubated with FITC-conjugated fibrinogen or PE/Cy5-conjugated
193 anti-human CD62P for 30 minutes. This was then diluted 25 x with Tyrodes-HEPES
194 buffer and read using a BD Accuri C6 plus flow cytometer. Platelets were gated
195 according to forward and size scatter and analysed using the BD Accuri software.

196

197 **7. Calcium measurement**

198 Human PRP was incubated with 2 μM Fura-2 AM for 1 hour at 30°C. PRP
199 was centrifuged at 350 *g* for 20 minutes and WP (4 x 10^8 platelets/mL) resuspended in
200 Tyrodes-HEPES buffer. Platelets were immediately placed in a 96-wells black plate
201 with clear bottom and incubated with 3.75 μM Bepristat and/or 3 μM ML171 for 10
202 minutes and stimulated with 1 μg/mL CRP. Fluorescence was read every 5 seconds

203 for 5 minutes using a Flexstation 3 fluorimeter (excitation 340 and 380 and emission
204 510 nm). Calcium signal was derived from the ratio of the 340 and 380 excitation
205 beams.
206
207 **8. Platelet spreading**
208 Human WP (2 x 10^7 platelets/mL) were incubated with Bepristat (7.5 to 30
209 μM) and/or ML171 (0.1875 to 6 μM) for 10 minutes and left to adhere to collagen (30
210 μg/mL), fibrinogen (30 μg/mL) or CRP (10 μg/mL)-coated surfaces (96-wells plate)
211 for 45 minutes at 37°C. Non-adherent platelets were washed off three times with PBS.
212 Paraformadehyde 0.2% was added for 10 minutes to fix the platelets. Triton-X 0.01%
213 v/v was added for 5 minutes to permeabilize the cells. After three washes with PBS to
214 remove Triton-X, platelets were stained with Alexa Fluor 488-conjugated phalloidin
215 (1:1000 v/v) for 1 hour in the dark at room temperature and analyzed using a 20x lens
216 on a Nikon A1-R Confocal microscope.
217
218 **9. Immunoblotting**
219 Human WP (4 x 10^8 platelets/mL) were incubated with 15 μM Bepristat
220 and/or 3 μM ML171 for 10 minutes and stimulated with 3 μg/mL collagen. On some
221 experiments, collagen was not added in order to assess the effects of PDI and Nox-1
222 inhibitors in resting platelets. For mouse experiments, WP (2 x 10^8 platelets/mL) were
223 incubated with 7.5 μM Bepristat for 10 minutes and stimulated with 5 μg/mL
224 collagen. Platelets were lysed in reducing Laemmli buffer (12% (w/v) Sodium
225 Dodecyl Sulphate (SDS), 30% (v/v) glycerol, 0.15 M Tris-HCl (pH 6.8), 0.001%
226 (w/v) Brilliant Blue R, 30% (v/v) β-mercaptoethanol) and heated for five to ten
227 minutes. SDS-PAGE and immunoblotting were performed using standard protocols
228 exactly as described in [2]. Specific primary phosphor-antibodies were used as
229 described in figure legends. Mouse anti-human GAPDH was used as loading controls.
230 Membranes were visualised using a Typhoon imaging system (GE Healthcare,
231 Hatfield, UK). For experiments using PKC substrate and 4G10 antibodies, all
232 phosphorylated bands were normalized to the corresponding GAPDH band.
233
234 **10. Tail bleeding assay**
235 Nox-$1^{-/-}$ or C57BL/6 wildtype (WT) mice were anesthesized through an
236 intraperitoneal injection of ketamine (100 mg/kg) and xylazine (10 mg/kg). After

237 animals were fully anaesthetized, Bepristat (0.5 μL of a 100 μM solution diluted in
238 100 μL PBS per 25 g of animal; 50 μM *in vivo* concentration) was injected
239 intravenously. After 5 minutes, 5 mm of the tail was amputated using a sharp blade.
240 The bleeding tail was then placed in PBS buffer kept at 37 °C and bleeding time
241 recorded for up to 20 minutes, after which mice were terminated.
242
243 **11. Population study**
244 This study comprised of 136 volunteers aged 30 to 65 not using chronic
245 medications that were recruited at the University of Reading to assess physical,
246 metabolic and platelet characteristics. Volunteers answered a questionnaire about
247 their age, gender, amongst other questions not included in this study. A competent
248 researcher measured the height, weight, body mass index (BMI) blood pressure (BP,
249 measured seated with an electronic automatic sphygmomanometer) and waist and hip
250 circumferences. Blood was taken after overnight fasting and serum glucose levels
251 measured using standard biochemistry protocols. Platelets were washed and
252 immunoblotting performed as above. Loading control GAPDH was used to normalize
253 levels of PDI and Nox-1 to protein loading in each well.
254 Volunteers were stratified according to their BMI as healthy weight (18.5 –
255 24.9 kg/m^2), overweight (25 – 29 kg/m^2), class 1 obesity (30 – 34.9 kg/m^2) and class 2
256 obesity (35 – 39.9 kg/m^2). BP was stratified according to the International Society of
257 hypertension [4]: normal (systolic <130 and diastolic <85 mmHg), high-normal
258 (systolic 130-139 and/or diastolic 85-89 mmHg), grade 1 hypertension (systolic 140-
259 159 and/or diastolic 90-99 mmHg) and grade 2 hypertension (systolic ≥160 and/or
260 diastolic ≥100 mmHg). Glycaemia was stratified according to the American Diabetes
261 Association [5]: normoglycaemia (<5.6 mmol/L), impaired fasting glycaemia (IFG) (5.6
262 – 6.9 mmol/L) and hyperglycaemia (>6.9 mmol/L). Waist circumference was
263 stratified according to the European Society of Cardiology [6]: normal (Caucasian men
264 <94 cm; men of other ethnicities <90 cm; women <80 cm) and central obesity
265 (Caucasian men ≥94 cm; men of other ethnicities ≥90 cm; women ≥80 cm).
266
267 **12. Statistical analysis**
268 Statistical analyses were performed on GraphPad Prism 8.0 software
269 (GraphPad Software, San Diego, USA). Bar graphs and tables express mean ± SEM.
270 Sample size varied from 4-6 independent repeats for *in vitro* experiments and between

271 6 and 8 for tail bleeding experiments. Outliers were determined and excluded by
272 ROUT test. For *in vitro* experiments using inhibitors, statistical analysis was
273 performed through paired one-way ANOVA and Tukey as post-test, whereas for *in*
274 *vivo* experiments using Nox-1$^{-/-}$ mice, these were analysed through two-way ANOVA
275 and Sidak's multiple comparisons test.

276 For the population study, linear regression was used to assess the correlation
277 between platelet PDI and Nox-1 levels. To assess the possible association of platelet
278 Nox-1 and PDI with risk factors for metabolic syndrome, volunteers were stratified
279 according to their BMI, BP, waist circumference and glycaemia. Analysis was
280 performed through unpaired one-way ANOVA and Tukey as post-test.

281

282 **REFERENCES**

283 1. Sousa HR, Gaspar RS, Sena EM, da Silva SA, Fontelles JL, AraUjo TL, Mastrogiovanni M,
284 Fries DM, Azevedo-Santos AP, Laurindo FR, Trostchansky A, Paes AM. Novel antiplatelet
285 role for a protein disulfide isomerase-targeted peptide: Evidence of covalent binding to the c-
286 terminal cghc redox motif. *J Thromb Haemost*. 2017;15:774-784

287 2. Gaspar RS, da Silva SA, Stapleton J, Fontelles JLL, Sousa HR, Chagas VT, Alsufyani S,
288 Trostchansky A, Gibbins JM, Paes AMA. Myricetin, the main flavonoid in syzygium cumini
289 leaf, is a novel inhibitor of platelet thiol isomerases pdi and erp5. *Front Pharmacol*.
290 2019;10:1678

291 3. Bye AP, Unsworth AJ, Desborough MJ, Hildyard CAT, Appleby N, Bruce D, Kriek N, Nock
292 SH, Sage T, Hughes CE, Gibbins JM. Severe platelet dysfunction in nhl patients receiving
293 ibrutinib is absent in patients receiving acalabrutinib. *Blood Adv*. 2017;1:2610-2623

294 4. Unger T, Borghi C, Charchar F, Khan NA, Poulter NR, Prabhakaran D, Ramirez A, Schlaich
295 M, Stergiou GS, Tomaszewski M. 2020 international society of hypertension global
296 hypertension practice guidelines. *Hypertension*. 2020;75:1334-1357

297 5. Association AD. 2. Classification and diagnosis of diabetes: Standards of medical care in
298 diabetes—2019. *Diabetes care*. 2019;42:S13-S28

299 6. Mach F, Baigent C, Catapano AL, Koskinas KC, Casula M, Badimon L, Chapman MJ, De
300 Backer GG, Delgado V, Ference BA. 2019 esc/eas guidelines for the management of
301 dyslipidaemias: Lipid modification to reduce cardiovascular risk. *Atherosclerosis*.
302 2019;290:140-205

303